Published in final edited form as:
J Immunol. 2013 May 15; 190(10): 5078–5085. doi:10.4049/jimmunol.1203228.

CD43-mediated IFN-γ production by CD8+ T cells promotes abdominal aortic aneurysm in mice

Hui-fang Zhou[*], **Huimin Yan**[*], **Judy L. Cannon**[†], **Luke E. Springer**[*], **Jonathan M. Green**[‡], and **Christine T.N. Pham**[*]

[*]Department of Medicine, Division of Rheumatology, Washington University School of Medicine, Saint Louis, MO 63110, USA

[†]Departments of Molecular Genetics and Microbiology and Pathology, University of New Mexico Health Sciences Center, Albuquerque, NM 87131, USA

[‡]Department of Medicine, Division of Pulmonary and Critical Care, Washington University School of Medicine, Saint Louis, MO 63110, USA

Abstract

CD43 is a glycosylated surface protein abundantly expressed on lymphocytes. Its role in immune responses has been difficult to clearly establish, with evidence supporting both costimulatory and inhibitory functions. In addition, its contribution to disease pathogenesis remains elusive. Using a well-characterized murine model of elastase-induced abdominal aortic aneurysm (AAA) that recapitulates many key features of the human disease we established that the presence of CD43 on T cells is required for AAA formation. Moreover, we found that IFN-γ producing $CD8^+$ T cells, but not $CD4^+$ T cells, promote the development of aneurysm by enhancing cellular apoptosis and matrix metalloprotease activity. Reconstitution with IFN-γ producing $CD8^+$ T cells or recombinant IFN-γ promotes the aneurysm phenotype in $CD43^{-/-}$ mice while IFN-γ antagonism abrogates disease in WT animals. Furthermore we showed that the presence of CD43 with an intact cytoplasmic domain capable of binding to ezrin-radixin-moesin cytoskeletal proteins is essential for optimal *in vivo* IFN-γ production by T cells and aneurysm formation. We have thus identified a robust physiologic role for CD43 in a relevant animal model and established an important *in vivo* function for CD43-dependent regulation of IFN-γ production. These results further suggest that IFN-γ antagonism or selective blockade of $CD43^+CD8^+$ T cell activities merits further investigation for immunotherapy in AAA.

Introduction

CD43 (leukosialin, sialophorin), a transmembrane glycoprotein highly expressed on various hematopoietic cells and has been extensively linked to various T cell activities and functions. A costimulatory function of CD43 was suggested following early observation that T cells from patients with Wiskott-Aldrich syndrome, an X-linked recessive immunodeficiency disorder, have altered or defective CD43 expression that accompanies defects in cytotoxic and helper T-cell functions (1, 2). However, CD43-deficient murine T cells were subsequently found to have increased proliferation to various stimuli and augmented cytotoxic T cell response, leading to the conclusion that CD43 negatively regulates T cell adhesion and activation (3).

Correspondence: Christine T.N. Pham, 660 South Euclid Avenue, Box 8045, Saint Louis, MO 63110. Tel: 314-362-9043. Fax: 314-454-1091. cpham@dom.wustl.edu.

The predominant model for CD43 function is that the large, negatively charged extracellular domain sterically impedes formation of an effective immunologic synapse. However, subsequent studies have demonstrated that the negative regulatory function of CD43 depends on its intracellular domain (4, 5). Phosphorylation of CD43 cytoplasmic tail leads to its association with ezrin-radixin-moesin (ERM) cytoskeletal proteins and full T cell activation while inhibition of CD43 interaction with ERM proteins results in decreased cytokine production (6–8). These findings are in agreement with reports showing that signaling through CD43 increases T-bet expression and inhibits GATA-3 gene transcription, predisposing T cells toward a Th1 lineage commitment and inducing IFN-γ expression (9–11). Conversely, CD43-deficient T cells preferentially differentiate into Th2 cells that produce high levels of IL-4, IL-5, and IL-13 (12). Congruent with these findings, CD43-deficient mice exhibit increased inflammation in Th2-mediated allergic airway diseases. On the other hand, a preferential Th2 differentiation does not appear to clearly afford protection against Th1-mediated disease in non-obese diabetic mice or experimental autoimmune encephalomyelitis (EAE) (12), although conclusions regarding the exact contribution of CD43 to disease phenotype in the EAE model remain contradictory (13, 14).

Abdominal aortic aneurysms (AAA) is a common vascular disease characterized by transmural inflammation of the aortic wall tissues, excessive local production of proteolytic enzymes (metalloproteases, MMPs) capable of degrading the extracellular matrix (ECM) and depletion/apoptosis of smooth muscle cells (SMCs), leading to the weakening and dilatation of the abdominal aorta (15). The inflammation in AAA is characterized by infiltration of the aortic wall with every type of leukocytes, including an abundance of lymphocytes (16). Greater than 50% of the lymphocytes recovered from AAA tissues are $CD3^+$ T cells, including $CD4^+$ and $CD8^+$ T cells (17). Thus, elucidating the mechanisms by which T cells contribute to the inflammatory environment may further our understanding of the mechanisms that underlie the destructive process in AAA.

T cells in AAA tissues can express both Th1 (IL-2, IFN-γ) and Th2 cytokines (IL-4, IL-10). While some reports suggest that Th1 cytokines are more consistently upregulated in large aneurysms (18–20) and expression of IFN-γ is increased in the circulation and in tissues of patients with AAA compared to controls (18, 20, 21) others suggest that a Th2 response predominates (22). Given its proposed costimulatory function, we wished to test the hypothesis that, by directing T cells toward a Th1 phenotype, CD43 promotes aneurysmal development. Herein, we show that CD43-deficiency confers complete resistance to elastase-induced AAA. In addition, we found that reconstitution with CD43-sufficient $CD8^+$ T cells restores susceptibility to aneurysm development through an IFN-γ-dependent but perforin-independent mechanism.

Materials and Methods

Animals

WT C57BL/6, C57BL/6-Ly5.1 (B6.SJL-*Ptprc*^{a}*Pepc*^{b}/BoyJ), perforin$^{-/-}$ (C57BL/6-*Pfp*^{tm1Sdz}), IFN-γ$^{-/-}$ (B6.129S7-*Ifng*^{tm1Ts}/J) and $CD8^{-/-}$ (B6.129S2-*Cd8a*^{tm1Mak}/J) mice were obtained from the Jackson Laboratory. $CD43^{-/-}$ mice were generously provided by Dr. Jonathan Green (3, 4). CD43-FL and CD43-NGG transgenic T cells were generously provided by Dr. Judy Cannon (8). All mice were kept in a pathogen free condition at Washington University Specialized Research Facility. All the experiments were performed according to protocols approved by the Division of Comparative Medicine.

Elastase perfusion model of AAA

AAA was induced as previously described. (23–25). Briefly, mice were anesthetized with 55–60 mg/kg i.p. sodium pentobarbital. A laparotomy was performed under sterile conditions. The abdominal aorta was isolated and the pre-perfused aortic diameter (AD) was measured with a calibrated ocular grid. Temporary 7-0 silk ligatures were placed around the proximal and distal aorta to interrupt proximal flow. An aortotomy was created at the inferior ligature using the tip of a 30-gauge needle and the aortic lumen was perfused for 5 min at 100 mm Hg with a solution containing 0.145 U/ml type 1 porcine pancreatic elastase (Sigma). After removal of the catheter, the aortotomy was repaired without constriction of the lumen to restore the flow. At d14, a second laparotomy was performed and the perfused segment of the abdominal aorta was re-exposed and measured *in situ* prior to euthanasia and tissue procurement. AD was assessed on d14 unless otherwise indicated. Some mice received purified T cells (7-10e6 cells i.v. on d1, 3 or 7 post-elastase perfusion), mouse rIFN-γ (50,000 U i.p. on d3, 6, 9, and 11 post-elastase perfusion, R&D Systems) or Armenian Hamster mAb to IFN-γ (250 μg i.p. on d3 and 9; clone H22 was generously provided by Drs. Robert Schreiber and Kathleen Sheehan, Washington University School of Medicine) (26).

Immunohistochemistry

Immunohistochemistry for elastin and actin was performed as previously described (23–25). Briefly mouse abdominal aorta was dissected, snap-frozen in OCT compound, and sectioned at 9 μm. Elastin was stained with Verhoeff-van Gieson (VVG) using an Accustain Elastic Stain Kit (Sigma). SMC content was evaluated using an alkaline phosphatase-conjugated antibody to alpha-smooth muscle actin (1:200 dilution, Sigma). Color was visualized using an alkaline phosphatase substrate kit (Vector Laboratories). Elastin degradation was graded on a scale of 1–4 as previously described (23–25): 1 = less than 25% degradation, 2 = 25–50% degradation, 3 = 50–75% degradation, 4 = greater than 75% degradation. SMC actin content was also graded on a scale of 1–4 (23–25): 1 = less than 25% loss, 2 = 25–50% loss, 3 = 50–75% loss, 4 = greater than 75% loss. Neutrophils, macrophages, and $CD3^+$ T cells were visualized with a biotinylated anti-Gr1 mAb (1:100 dilution, BD Biosciences), anti-Mac-3 mAb (1:200 dilution, Cedarlane Laboratories) and anti-CD3 mAb (1:100 dilution, BD Biosciences), respectively. $MMP\text{-}2^+$ and $MMP\text{-}9^+$ cells were visualized with a rabbit polyclonal anti-MMP-2 Ab (0.2 μg/ml, Novus Biologicals) and an anti-MMP-9 mAb (2 μg/ml, R&D Systems). Terminal deoxynucleotidyl transferase dUTP nick end labeling (TUNEL) assay was performed as recommended by the manufacturers (Milliprore). Data presented were derived from 6–9 serial cross-sections that spanned the entire abdominal aorta, 4–5 aortas per genotype or treatment.

T cell isolation and adoptive transfer

$CD3^+$, $CD4^+$, and $CD8^+$ T cells were isolated from spleens and lymph nodes by negative selection using Miltenyi Biotec Magnetic-Activated Cell Sorting (MACS) microbeads. Cell purity was consistently > 95%. Isolated cells (7e6 for $CD4^+$ and $CD8^+$, 1e7 for total $CD3^+$ T cells) were resuspended in 100 μl PBS and injected i.v. into mice on d3 and 7 after elastase perfusion.

In vitro stimulation of T cells

$CD8^+$ T cells (2e5/well) purified as above were activated with plate-bound anti-CD3 mAb (1 μg/ml, BD Biosciences) and soluble anti-CD28 mAb (5 μg/ml, BD Biosciences) in RPMI supplemented with 10% FBS in triplicates in 96-well plates. After 72 h, supernatants were harvested and assayed for IFN-γ and IL-10 by ELISA (R&D Systems).

In vivo competitive T cell recruitment

Ly5.2 WT and CD43$^{-/-}$ T cells (1e7 each) were mixed at a 1:1 ratio and injected i.v. into congenic Ly5.1 mice on d1 post elastase perfusion. Alternatively, CD43 transgenic (Tg) T cells were differentially labeled with either CFSE (5 μM) or PKH-26 (2 μM), mixed at 1:1 ratio (1e7 each) prior to transfer. On the indicated day, aortas were excised from below the renal arteries to above the femoral bifurcation, minced and digested as previously described (23). Single cell suspensions obtained were surface labeled for Ly5.1, Ly5.2, CD43, TCRβ, CD4, or CD8 (eBioscience) to distinguish donor (Ly5.2^{+} or CD43^{+} Tg) from recipient cells (Ly5.1^{+} or endogenous CD43^{-}) and analyzed by flow cytometry (FACSCalibur).

IFN-γ immunofluorescence image analysis

Cross sections of aortic tissues (9μm) were fixed in 4% paraformaldehyde, blocked in 8% BSA in PBS and incubated with a goat polyclonal Ab to mouse CD43 (1:50 dilution, Santa Cruz Biotechnology) followed by rhodamine conjugated donkey anti-goat Ab (1:100 dilution; Jackson ImmunoResearch) and FITC-conjugated IFN-γ (1:100 dilution; eBioscience). All images were visualized on a Nikon Eclipse fluorescence microscope and acquired with QCapture software using the same exposure time. Merged and single color images were loaded into ImageJ software (http://rsb.info.nih.gov/ij) for analysis. Threshold color of all images was set to the same hue/saturation/brightness. Using the brightness to filter the picture, positively stained areas were isolated by increasing the contrast between the color and background. This facilitates the selection of regions of interest (ROIs) by allowing ROIs to be selected easily with the wand tool. Double positive (CD43^{+}IFN-γ^{+}) cells were selected; single CD43^{-} cells were deselected. The ROIs were measured on the unfiltered images, normalized to the positive area and presented as integrated optical density (IntDen). Data were obtained from 6–8 fields per section and 6–9 sections per aorta.

In situ zymography

Non-fixed, frozen sections (9 μm) of day 14 aortas were incubated with a fluorogenic gelatin substrate (DQ gelatin at 0.1mg/ml, Molecular Probes) for 3 h at room temperature. For negative control, slides were incubated in the presence of 25 mM EDTA. The specific removal of essential divalent cations resulted in no detectable gelatinolytic activity. All images were visualized on a Nikon Eclipse fluorescence microscope and acquired with QCapture software. The images were analyzed by ImageJ software and gelatinase activity was normalized to the intensity of WT sections, which was set at 100%. Data represent 6–9 sections per aorta, 4–5 aortas per genotype/treatment.

Statistics

Comparisons between multiple groups were made by one-way ANOVA followed by Bonferroni's post-test to compare all groups of data. Data are presented as the mean ± SEM. $P<0.05$ were considered significant.

Results

CD43$^{-/-}$ mice are resistant to elastase-induced AAA

Transient porcine elastase perfusion of abdominal aorta is a widely used animal model of AAA that recapitulates many key features of the human disease histologically (27, 28). Immediately following intraluminal perfusion with elastase we observed the same extent of aortic diameter (AD) dilation in WT and CD43$^{-/-}$ mice (increase in AD of ~70%) (fig. 1A–B). This AD has previously been shown to remain relatively stable until d7 post-elastase perfusion, after which there was a rapid increase in WT animals (23). Aneurysm is defined on d14 as an increase in the AD of at least 100% or greater compared with the pre-perfused

parameters (28). The absence of CD43 protected mice from aneurysm development (increase in AD of 91.8 ± 6.2% or 0.44 ± 0.03 mm in $CD43^{-/-}$ animals vs. 144.8 ± 3.7% or 0.73 ± 0.1 mm in WT animals, $P < 0.0001$) (fig. 1A–B). Histologic analysis of d14 aortas revealed severe fragmentation of the elastic fibers and depletion of SMC actin in WT animals compared with the relatively well-preserved elastic lamellae and SMC actin content in $CD43^{-/-}$ animals (fig. 1C–E, $P < 0.0001$).

Normal neutrophil recruitment but blunted chronic inflammatory response in $CD43^{-/-}$ mice

As CD43 is implicated in cellular trafficking (29–31), we first assessed the acute neutrophil response to elastase perfusion in $CD43^{-/-}$ mice on d3. We found no difference in the number of neutrophils recruited to aortic wall between WT and $CD43^{-/-}$ mice (fig. 2A–B, $P > 0.05$). On the other hand, histologic analysis of day 14 aortas revealed significantly less Mac-3^+ macrophages ($P < 0.0001$) and $CD3^+$ T cells ($P < 0.0001$) in $CD43^{-/-}$ mice (fig. 2A, C–D). The lower $CD3^+$ T cell count reflects a decrease in both $CD4^+$ and $CD8^+$ T cells (fig. 3). On the other hand, NK cell number was relatively equivalent (946 ± 317 NK cells per WT aorta vs. 985 ± 240 NK cells per $CD43^{-/-}$ aorta, $P > 0.5$). Consistent with a lower number of $CD8^+$ T cells, we observed ~60% reduction in the apoptotic index, as measured by TUNEL staining (fig. 2A and E). Taken together, these results suggest that the absence of CD43 abrogates aneurysm development by dampening T cell and macrophage responses.

$CD8^+$ T cell reconstitution restores susceptibility to AAA development in $CD43^{-/-}$ mice

We next probed the contribution of T cells to aneurysm development. First, we reconstituted $CD43^{-/-}$ mice with total $CD3^+$ T cells. Reconstitution with WT $CD3^+$ T cells fully restored susceptibility to AAA in $CD43^{-/-}$ mice (increase in AD of 0.74 ± 0.02 mm WT T cell recipients vs. 0.43 ± 0.03 mm in $CD43^{-/-}$ T cell recipients, $P < 0.001$) (fig 4A). Next, we examined the contribution of $CD8^+$ vs. $CD4^+$ T cells. We found that reconstitution with WT $CD4^+$ T cells did not induce AAA formation in $CD43^{-/-}$ mice while reconstitution with WT $CD8^+$ T cells fully restored susceptibility to aneurysm development ($P < 0.001$) (fig. 4A). Reconstitution with WT $CD8^+$ T cells led to the characteristic severe fragmentation of the elastic fibers (fig. 4B) and depletion of SMC actin (fig. 4C). These results indicate that $CD8^+$ T cells promote the AAA phenotype and that CD43 expression on T cells is specifically required.

Absence of $CD8^+$ T cells attenuates aneurysm development

To further assess the specific contribution of $CD8^+$ T cells to the AAA phenotype, we examined mice that lack $CD8^+$ T cells ($CD8^{-/-}$). We confirmed that $CD8^{-/-}$ mice have significantly attenuated aneurysm phenotype (increase in AD of 108 ± 3.7% or 0.54 ± 0.02 mm in $CD8^{-/-}$ vs. 146.8 ± 5.4% or 0.74 ± 0.20 mm in WT animals, $P < 0.001$) (fig. 5A–B). The resistant phenotype was accompanied by relative preservation of elastic fiber integrity and SMC actin content (fig. 5C–D) and a decrease in the number of Mac-3^+ macrophages in the aortic wall tissues ($P < 0.001$) (fig. 5E). Reconstitution of $CD8^{-/-}$ mice with WT $CD8^+$ T cells restored the AAA phenotype while reconstitution with WT $CD4^+$ T cells did not (fig. 5A–B). $CD8^+$ T cell transfer also led an increase in the number of Mac-3^+ macrophages localizing to the arterial wall (fig. 5E), suggesting that $CD8^+$ T cells are necessary for normal macrophage recruitment and/or activation during AAA development.

Defective IFN-γ production by $CD8^+$ T cells protects $CD43^{-/-}$ mice against AAA

To determine whether a defect in T cell migration to the site of inflammation protects $CD43^{-/-}$ mice against AAA development we used the allelic markers Ly5.1 and Ly5.2 (32) to distinguish donor and recipient T cells after adoptive transfer. Isolated $CD8^+$T cells

(expressing Ly5.2) from WT and CD43$^{-/-}$ mice were mixed together (1:1 ratio) and transferred into congenic WT C57BL/6 mice expressing the allelic marker Ly5.1 on d1 post-elastase perfusion. On d3, donor T cells (expressing Ly5.2) were recovered from abdominal aorta digest and analyzed for the expression of CD43. We found that CD43$^{-/-}$ CD8^{+}T cells migrated to the elastase perfused aortic wall as efficiently as WT CD8^{+}T cells (fig. 6A), suggesting that the resistant phenotype cannot be explained by a defect in the initial recruitment of CD43$^{-/-}$ T cells to the elastase-perfused aorta.

In contrast, we found that CD43$^{-/-}$ CD8^{+}T cells had a significant defect in their ability to produce IFN-γ when activated *in vitro* with anti-CD3/CD28 mAb while IL-10 production was normal (fig. 6B). Given previous reported role of IFN-γ in experimental AAA (33) we hypothesized that IFN-γ production by CD8 $^{+}$ T cells is required for aneurysm formation. To test this hypothesis, we injected elastase-perfused CD43$^{-/-}$ mice with 50,000 U recombinant mouse IFN-γ on d3, 6, 9, and 11 post-perfusion. IFN-γ fully reconstituted the aneurysm phenotype in CD43$^{-/-}$ mice (fig. 7A) and led to the characteristic elastic fiber fragmentation (fig. 7B) and SMC actin depletion (fig. 7C). On the other hand, IFN-γ blockade with the mAb H22 (26, 34) abrogated AAA development in WT animals (fig. 7A). To specifically determine the contribution of IFN-γ producing CD8^{+} T cells in aneurysm development we reconstituted CD43$^{-/-}$ mice with IFN-γ$^{-/-}$CD8^{+} T cells. IFN-γ$^{-/-}$ CD8^{+} T cells failed to induce AAA in CD43$^{-/-}$ mice (fig. 7A). These results strongly indicate that IFN-γ produced by CD8^{+} T cells is required for elastase-induced AAA.

CD43 directs IFN-γ production in CD8^{+} T cells

The above data support that CD43^{+}CD8^{+} T cells induce aneurysm formation by elaborating IFN-γ. To further elucidate how CD43 signals regulate IFN-γ production in T cells, we turned to a well-characterized CD43 transgenic T cell model in which a mutation of the tripeptide KRR sequence within the intracellular domain of CD43 leads to a perturbation of its interaction with ERM proteins (5, 7, 8). Transfer of CD43-NGG Tg cells (that express a form of CD43 in which the KRR sequence was mutated to NGG) (8) into elastase-perfused CD43$^{-/-}$ mice did not lead to AAA development (fig. 8A). On the other hand, elastase-perfused CD43$^{-/-}$ mice that received CD43-FL Tg cells (that express the full length WT CD43) developed aneurysm at WT level (increase in AD of 0.44 ± 0.02 mm in CD43-NGG recipients vs. 0.77 ± 0.3 mm in CD43-FL recipients, $P < 0.001$) (fig. 8A). Histologic analysis of d14 aorta confirmed that reconstitution with CD43-FL Tg cells led to severe fragmentation of elastic fibers and loss of SMC actin in CD43$^{-/-}$ recipient mice (data not shown).

Previous studies showed that perturbation of CD43 intracellular domain interaction with ERM proteins significantly decreases cytokine production (5, 7). Indeed we confirmed that CD43-NGG Tg cells that migrated to the aortic wall of CD43$^{-/-}$ mice expressed ~55% less IFN-γ when compared to CD43-FL cells Tg cells (fig. 8B and fig. S1, $P < 0.001$). In addition, when we examined the CD43 Tg cells that migrated to the abdominal para-aortic lymph nodes of reconstituted mice we also found a significant reduction in the percentage of CD43-NGG CD8^{+} T cells expressing IFN-γ as well as a decrease in the actual level of IFN-γ (fig. S2).

Since a previous report also showed that CD43-NGG cells have a defect in their ability to traffic to lymph nodes (8), we wanted to determine whether resistance to aneurysm development in CD43$^{-/-}$ mice that received CD43-NGG cells could be due to a defect in Tg cell recruitment. CD43-FL and CD43-NGG Tg cells were differentially labeled with fluorescent dyes, mixed at 1:1 ratio and transferred to elastase-perfused recipients. Analysis of cells recovered from digested samples confirmed that the numbers of CD43-FL and CD43-NGG Tg cells recruited to elastase-perfused aortas at 20 h were equivalent (fig. 8C).

Taken together, the results above support the concept that CD43 intracellular domain is required for the optimal production of IFN-γ and AAA genesis.

IFN-γ promotes cellular apoptosis *in vivo*

An important role proposed for $CD8^+$ T cells in AAA is the mediation of SMC apoptosis, possibly through the perforin/granzyme granule exocytosis pathway (35). To determine the contribution of perforin in elastase-induced AAA, we examined the perforin-deficient ($Pfp^{-/-}$) mice (36, 37) and found that they were as susceptible to elastase-induced AAA as WT animals (data not shown). Moreover, reconstitution of $CD43^{-/-}$ mice with $Pfp^{-/-}$ $CD8^+$ T cells fully restored the AAA phenotype (fig. 7A). Consistent with the susceptible phenotype we found that reconstitution of $CD43^{-/-}$ mice with $Pfp^{-/-}$ $CD8^+$ T cells led to significant elastic fiber degradation and SMC depletion (fig. 7B–C). Moreover, we observed that reconstitution of $CD43^{-/-}$ mice with $Pfp^{-/-}$ $CD8^+$ T cells or IFN-γ led to a significant increase in the apoptotic index ($P < 0.001$) while reconstitution with IFN-$\gamma^{-/-}$ $CD8^+$ T cells did not (fig. 7D). Taken together, these results suggest that $CD8^+$ T cells promote *in vivo* cellular apoptosis through an IFN-γ-dependent pathway while perforin-dependent cytotoxicity is dispensable.

IFN-γ released by $CD8^+$ T cells promotes MMP-producing macrophage recruitment

MMPs released by macrophages are thought to be responsible for local tissue destruction and the eventual aneurysmal dilatation (38). To understand whether IFN-γ modulates the local production and activity of MMPs, we first examined d14 aortas from WT and $CD43^{-/-}$ mice. We observed that the number of Mac-3^+ along with MMP-2^+ and MMP-9^+ cells infiltrating the aortic wall tissues were significantly lower in $CD43^{-/-}$ mice ($P < 0.001$) (fig. 9A–D) as was the local gelatinase activity detected by *in situ* zymography, confirming that MMP activity was greatly attenuated in $CD43^{-/-}$ aortas (29% of WT level, $P < 0.01$) (fig. 9E–F). Reconstitution of $CD43^{-/-}$ mice with WT $CD8^+$ T cells or IFN-γ increased the number of Mac-3^+, MMP-2^+ and MMP-9^+ cells ($P < 0.001$) (fig. 9B–D) and enhanced local gelatinase activity (95% and 98% of WT level respectively, $P < 0.01$) (fig. 9F) while reconstitution of $CD43^{-/-}$ mice with IFN-$\gamma^{-/-}$ $CD8^+$ T cells did not. Taken together, these results suggest that IFN-γ produced by CD43 $^+CD8^+$ T cells likely promotes the recruitment (or expansion) of MMP-producing macrophages and enhances the local MMP activity, all of which likely contribute to ECM degradation.

Discussion

The findings herein offer new insights into the role of CD43 in a relevant disease model that recapitulates key features of human AAA in many aspects. We showed that the presence of CD43 with an intact cytoplasmic domain capable of binding to ERM proteins is essential for IFN-γ production by $CD8^+$ T cells and aneurysm formation. Moreover, we established an essential role for $CD8^+$ T cells in AAA genesis. Although $CD8^+$ T cells have long been implicated in the apoptosis of SMCs, a direct pathogenic role for these cells in AAA has not been established. Our data also suggest that IFN-γ elaborated by $CD8^+$ T cells suffices to induce apoptosis *in vivo* while perforin of the granule exocytosis pathway is dispensable. Conversely, blockade of IFN-γ activity abrogates aneurysm formation. IFN-γ released by activated $CD8^+$ T cells promotes local tissue destruction through the recruitment/expansion of MMP-producing macrophages.

Although CD43 has been linked to many T cell activities (3, 9–11, 30, 39–41), its physiologic contribution to T cell functions in inflammation and diseases remains a point of debate. Previous studies have shown that the absence of CD43 results in a preferential Th2 differentiation and the exacerbation of Th2-mediated diseases (12). And although a Th2-

biased response suggests that CD43$^{-/-}$ mice should be protected against Th1-mediated diseases (such as EAE), the reports thus far present conflicting results, ranging from no differences in disease phenotype (12) to partial protection against disease induction (13, 14). Herein we used the elastase-induced AAA model to establish that CD43 expression is required for CD8^{+} T cell activation and enhances IFN-γ production *in vivo*. A defect in IFN-γ production by CD43$^{-/-}$ T cells is not routinely described. However, CD43 interaction with ERM proteins is well documented and was previously mapped to the KRR sequence motif within the intracellular domain of CD43. Mutations of these residues perturb the interaction of CD43 with ERM proteins blocking its accumulation at a pole complex distal to the immune synapse and diminishing the production of multiple cytokines in T cells, including IFN-γ (5–7). In addition, a recent report demonstrates that the organization of this distal pole complex is required for optimal T cell activation as conditional deletion of ezrin, in combination with small interfering RNA (siRNA) suppression of moesin, disrupts normal Ca^{2+} flux and phospholipase C-γ1 activation and diminishes cytokine gene expression in T cells (42). Taken together, these results suggest that in the CD43-NGG Tg adoptive transfer model the ability of CD8^{+} Tg cells to induce the aneurysm phenotype is directly related to the interactions mediated by the cytoplasmic tail of CD43 with ERM proteins, the colocalization of which is required for optimal T cell activation and IFN-γ production (7, 42). Furthermore we confirmed *in vivo* that the number of CD43$^{-/-}$ and CD43-NGG Tg cells initially recruited to the elastase-perfused aorta is comparable to that of WT and CD43-FL, thus ruling out a defect in T cell trafficking as the mechanism underlying disease resistance. The normal initial T cell recruitment further suggests that the reduction in T cell number observed on d14 in CD43$^{-/-}$ aortic sections may reflect an imbalance in cell homeostasis/survival in the absence of CD43, consistent with previous studies suggesting that CD43 has an anti-apoptotic function (43), or that CD43$^{-/-}$ T cells may be less capable of expansion (30).

The finding that only CD8^{+} T cells restore the aneurysmal phenotype in CD43$^{-/-}$ mice was unexpected. However, these data do not negate the previously established role for CD4^{+} T cells in $CaCl_2$-induced AAA (33). Instead, our data suggest a hierarchal order with which T cells are activated and IFN-γ is produced during elastase-induced AAA development. The magnitude and rapidity with which activated CD8^{+} T cells initiate IFN-γ production in the early phase of the immune response likely explain their immunodominant role in further directing lineage commitment and expansion of that subset and surrounding leukocytes, including naïve CD4^{+} T cells. This immunodominance of IFN-γ producing CD8^{+} T cells during immune responses has previously been established in other model systems (44–46). However, the fact that CD43$^{-/-}$ mice have a slightly more resistant AAA phenotype (i.e. smaller AD on day 14 following elastase perfusion) than mice that are deficient only in CD8^{+} T cells suggests that CD43 expression on other leukocyte subsets, including CD4^{+} T cells, may indeed contribute to the overall AAA phenotype downstream of CD8^{+} T cell activation.

The finding that IFN-γ directs the inflammatory cascade in the elastase-induced AAA model is in agreement with a report by Xiong *et al* (33). It stands, hovever, in stark contrast to other published studies. In the study by Shimizu *et al.*, the authors reported that aortic allografts transplanted into IFN-γ receptor null mice developed into severe AAA with a T2-predominant inflammation (47). Likewise, King *et al.*, using an apolipoprotein E- and IFN-γ-deficient model, showed that IFN-γ protects against aneurysm formation and rupture (48). Although we cannot reconcile these divergent findings, it should be noted that these models differ significantly from the elastase perfusion model used herein. In addition, the Shimizu *et al.* and King *et al.* studiesemployed models in which IFN-γ and IFN-γ receptor were absent throughout the animals' development whereas the IFN-γ deficiency in the CD43$^{-/-}$ mice is only relative. Thus IFN-γ may have a dynamic effect on T cells (and likely other

leukocytes) that may be stimulatory or protective over the course of an immune response, depending on the level and the timing of its expression.

In summary, we have identified a robust phenotype for the CD43-deficient mouse and established an important *in vivo* function for CD43-dependent regulation of IFN-γ production. Our results indicate that interactions mediated by the intracellular domain of CD43 in $CD8^+$ T cells induce the production of IFN-γ that in turn orchestrates an inflammatory cascade, leading to the eventual aneurysmal degeneration. In addition we have demonstrated for the first time a direct role for $CD43^+CD8^+$ T cells in the pathogenesis of AAA. Distinct populations of $CD8^+$ T cells expressing different glycoforms of CD43 and possessing differential cytotoxic activity have been described in a model of murine intestinal inflammation (49). Whether these subpopulations of $CD43^+CD8^+$ T cells exist in humans and in AAA remains to be determined. Nonetheless, these studies and our results further suggest that IFN-γ and CD43 represent potential targets for immunotherapy in AAA and that selective depletion or blockade of $CD43^+CD8^+$ T cell activities merits further investigation as it may have beneficial effects in other IFN-γ- and $CD8^+$ T-cell-dependent diseases.

Supplementary Material

Refer to Web version on PubMed Central for supplementary material.

Acknowledgments

The authors would like to acknowledge Ying Hu for excellent technical assistance. We thank Drs. Robert Schreiber and Kathleen Sheehan for the generous gift of anti-IFN-γ monoclonal antibody.

This work was supported by NIH grants AI049261 and AR056468 to C.T.N.P. and American Heart Association Scientist Development Grant 09SDG2260379 to J.L.C.

References

1. Remold-O'Donnell E, Rosen FS. Sialophorin (CD43) and the Wiskott-Aldrich syndrome. Immunodefic Rev. 1990; 2:151–174. [PubMed: 2223062]
2. Park JK, Rosenstein YJ, Remold-O'Donnell E, Bierer BE, Rosen FS, Burakoff SJ. Enhancement of T-cell activation by the CD43 molecule whose expression is defective in Wiskott-Aldrich syndrome. Nature. 1991; 350:706–709. [PubMed: 2023632]
3. Manjunath N, Correa M, Ardman M, Ardman B. Negative regulation of T-cell adhesion and activation by CD43. Nature. 1995; 377:535–538. [PubMed: 7566153]
4. Walker J, Green JM. Structural requirements for CD43 function. J Immunol. 1999; 162:4109–4114. [PubMed: 10201935]
5. Tong J, Allenspach EJ, Takahashi SM, Mody PD, Park C, Burkhardt JK, Sperling AI. CD43 regulation of T cell activation is not through steric inhibition of T cell-APC interactions but through an intracellular mechanism. J Exp Med. 2004; 199:1277–1283. [PubMed: 15117976]
6. Delon J, Kaibuchi K, Germain RN. Exclusion of CD43 from the immunological synapse is mediated by phosphorylation-regulated relocation of the cytoskeletal adaptor moesin. Immunity. 2001; 15:691–701. [PubMed: 11728332]
7. Allenspach EJ, Cullinan P, Tong J, Tang Q, Tesciuba AG, Cannon JL, Takahashi SM, Morgan R, Burkhardt JK, Sperling AI. ERM-dependent movement of CD43 defines a novel protein complex distal to the immunological synapse. Immunity. 2001; 15:739–750. [PubMed: 11728336]
8. Cannon JL, Mody PD, Blaine KM, Chen EJ, Nelson AD, Sayles LJ, Moore TV, Clay BS, Dulin NO, Shilling RA, Burkhardt JK, Sperling AI. CD43 interaction with ezrin-radixin-moesin (ERM) proteins regulates T-cell trafficking and CD43 phosphorylation. Mol Biol Cell. 2011; 22:954–963. [PubMed: 21289089]

9. Mattioli I, Dittrich-Breiholz O, Livingstone M, Kracht M, Schmitz ML. Comparative analysis of T-cell costimulation and CD43 activation reveals novel signaling pathways and target genes. Blood. 2004; 104:3302–3304. [PubMed: 15280197]
10. Montufar-Solis D, Garza T, Klein JR. Selective upregulation of immune regulatory and effector cytokine synthesis by intestinal intraepithelial lymphocytes following CD43 costimulation. Biochem Biophys Res Commun. 2005; 338:1158–1163. [PubMed: 16246302]
11. Ramirez-Pliego O, Escobar-Zarate DL, Rivera-Martinez GM, Cervantes-Badillo MG, Esquivel-Guadarrama FR, Rosas-Salgado G, Rosenstein Y, Santana MA. CD43 signals induce Type One lineage commitment of human CD4+ T cells. BMC Immunol. 2007; 8:30. [PubMed: 18036228]
12. Cannon JL, Collins A, Mody PD, Balachandran D, Henriksen KJ, Smith CE, Tong J, Clay BS, Miller SD, Sperling AI. CD43 regulates Th2 differentiation and inflammation. J Immunol. 2008; 180:7385–7393. [PubMed: 18490738]
13. Ford ML, Onami TM, Sperling AI, Ahmed R, Evavold BD. CD43 modulates severity and onset of experimental autoimmune encephalomyelitis. J Immunol. 2003; 171:6527–6533. [PubMed: 14662853]
14. Ford ML, Evavold BD. Modulation of MOG 37–50-specific CD8+ T cell activation and expansion by CD43. Cell Immunol. 2006; 240:53–61. [PubMed: 16890924]
15. Thompson RW, Geraghty PJ, Lee JK. Abdominal aortic aneurysms: basic mechanisms and clinical implications. Curr Probl Surg. 2002; 39:110–230. [PubMed: 11884965]
16. Kuivaniemi H, Platsoucas CD, Tilson MD 3rd. Aortic aneurysms: an immune disease with a strong genetic component. Circulation. 2008; 117:242–252. [PubMed: 18195185]
17. Forester ND, Cruickshank SM, Scott DJ, Carding SR. Functional characterization of T cells in abdominal aortic aneurysms. Immunology. 2005; 115:262–270. [PubMed: 15885133]
18. Galle C, Schandene L, Stordeur P, Peignois Y, Ferreira J, Wautrecht JC, Dereume JP, Goldman M. Predominance of type 1 CD4+ T cells in human abdominal aortic aneurysm. Clin Exp Immunol. 2005; 142:519–527. [PubMed: 16297165]
19. Middleton RK, Lloyd GM, Bown MJ, Cooper NJ, London NJ, Sayers RD. The pro-inflammatory and chemotactic cytokine microenvironment of the abdominal aortic aneurysm wall: a protein array study. J Vasc Surg. 2007; 45:574–580. [PubMed: 17321344]
20. Golledge AL, Walker P, Norman PE, Golledge J. A systematic review of studies examining inflammation associated cytokines in human abdominal aortic aneurysm samples. Dis Markers. 2009; 26:181–188. [PubMed: 19729799]
21. Juvonen J, Surcel HM, Satta J, Teppo AM, Bloigu A, Syrjala H, Airaksinen J, Leinonen M, Saikku P, Juvonen T. Elevated circulating levels of inflammatory cytokines in patients with abdominal aortic aneurysm. Arterioscler Thromb Vasc Biol. 1997; 17:2843–2847. [PubMed: 9409264]
22. Chan WL, Pejnovic N, Liew TV, Hamilton H. Predominance of Th2 response in human abdominal aortic aneurysm: mistaken identity for IL-4-producing NK and NKT cells? Cell Immunol. 2005; 233:109–114. [PubMed: 15963967]
23. Pagano MB, Bartoli MA, Ennis TL, Mao D, Simmons PM, Thompson RW, Pham CT. Critical role of dipeptidyl peptidase I in neutrophil recruitment during the development of experimental abdominal aortic aneurysms. Proc Natl Acad Sci U S A. 2007; 104:2855–2860. [PubMed: 17301245]
24. Pagano MB, Zhou HF, Ennis TL, Wu X, Lambris JD, Atkinson JP, Thompson RW, Hourcade DE, Pham CT. Complement-dependent neutrophil recruitment is critical for the development of elastase-induced abdominal aortic aneurysm. Circulation. 2009; 119:1805–1813. [PubMed: 19307471]
25. Zhou HF, Yan H, Stover CM, Fernandez TM, Rodriguez de Cordoba S, Song WC, Wu X, Thompson RW, Schwaeble WJ, Atkinson JP, Hourcade DE, Pham CT. Antibody directs properdin-dependent activation of the complement alternative pathway in a mouse model of abdominal aortic aneurysm. Proc Natl Acad Sci U S A. 2012; 109:E415–422. [PubMed: 22308431]
26. Buchmeier NA, Schreiber RD. Requirement of endogenous interferon-gamma production for resolution of Listeria monocytogenes infection. Proc Natl Acad Sci U S A. 1985; 82:7404–7408. [PubMed: 3933006]

27. Anidjar S, Salzmann JL, Gentric D, Lagneau P, Camilleri JP, Michel JB. Elastase-induced experimental aneurysms in rats. Circulation. 1990; 82:973–981. [PubMed: 2144219]
28. Thompson RW, Curci JA, Ennis TL, Mao D, Pagano MB, Pham CT. Pathophysiology of abdominal aortic aneurysms: insights from the elastase-induced model in mice with different genetic backgrounds. Ann N Y Acad Sci. 2006; 1085:59–73. [PubMed: 17182923]
29. McEvoy LM, Sun H, Frelinger JG, Butcher EC. Anti-CD43 inhibition of T cell homing. J Exp Med. 1997; 185:1493–1498. [PubMed: 9126930]
30. Onami TM, Harrington LE, Williams MA, Galvan M, Larsen CP, Pearson TC, Manjunath N, Baum LG, Pearce BD, Ahmed R. Dynamic regulation of T cell immunity by CD43. J Immunol. 2002; 168:6022–6031. [PubMed: 12055210]
31. Mody PD, Cannon JL, Bandukwala HS, Blaine KM, Schilling AB, Swier K, Sperling AI. Signaling through CD43 regulates CD4 T-cell trafficking. Blood. 2007; 110:2974–2982. [PubMed: 17638845]
32. Shen FW, Tung JS, Boyse EA. Further definition of the Ly-5 system. Immunogenetics. 1986; 24:146–149. [PubMed: 3489673]
33. Xiong W, Zhao Y, Prall A, Greiner TC, Baxter BT. Key roles of CD4+ T cells and IFN-gamma in the development of abdominal aortic aneurysms in a murine model. J Immunol. 2004; 172:2607–2612. [PubMed: 14764734]
34. Shreiber RD, Hicks LJ, Celada A, Buchmeier NA, Gray PW. Monoclonal antibodies to murine gamma-interferon which differentially modulate macrophage activation and antiviral activity. J Immunol. 1985; 134:1609–1618. [PubMed: 2578513]
35. Voskoboinik I, Dunstone MA, Baran K, Whisstock JC, Trapani JA. Perforin: structure, function, and role in human immunopathology. Immunol Rev. 2010; 235:35–54. [PubMed: 20536554]
36. Lowin B, Beermann F, Schmidt A, Tschopp J. A null mutation in the perforin gene impairs cytolytic T lymphocyte- and natural killer cell-mediated cytotoxicity. Proc Natl Acad Sci U S A. 1994; 91:11571–11575. [PubMed: 7972104]
37. Lowin B, Hahne M, Mattmann C, Tschopp J. Cytolytic T-cell cytotoxicity is mediated through perforin and Fas lytic pathways. Nature. 1994; 370:650–652. [PubMed: 7520535]
38. Thompson RW, Holmes DR, Mertens RA, Liao S, Botney MD, Mecham RP, Welgus HG, Parks WC. Production and localization of 92-kilodalton gelatinase in abdominal aortic aneurysms. An elastolytic metalloproteinase expressed by aneurysm-infiltrating macrophages. J Clin Invest. 1995; 96:318–326. [PubMed: 7615801]
39. Mosley RL, Hamad M, Whetsell M, Klein JR. A novel marker of murine bone marrow hematopoietic stem cells that is expressed on peripheral T cells and is associated with a functionally important molecule on activated cytotoxic T lymphocytes. Hybridoma. 1994; 13:353–358. [PubMed: 7860091]
40. Sperling AI, Green JM, Mosley RL, Smith PL, DiPaolo RJ, Klein JR, Bluestone JA, Thompson CB. CD43 is a murine T cell costimulatory receptor that functions independently of CD28. J Exp Med. 1995; 182:139–146. [PubMed: 7790813]
41. Woodman RC, Johnston B, Hickey MJ, Teoh D, Reinhardt P, Poon BY, Kubes P. The functional paradox of CD43 in leukocyte recruitment: a study using CD43-deficient mice. J Exp Med. 1998; 188:2181–2186. [PubMed: 9841931]
42. Shaffer MH, Dupree RS, Zhu P, Saotome I, Schmidt RF, McClatchey AI, Freedman BD, Burkhardt JK. Ezrin and moesin function together to promote T cell activation. J Immunol. 2009; 182:1021–1032. [PubMed: 19124745]
43. Seo W, Ziltener HJ. CD43 processing and nuclear translocation of CD43 cytoplasmic tail are required for cell homeostasis. Blood. 2009; 114:3567–3577. [PubMed: 19696198]
44. Rodriguez F, Harkins S, Slifka MK, Whitton JL. Immunodominance in virus-induced CD8(+) T-cell responses is dramatically modified by DNA immunization and is regulated by gamma interferon. J Virol. 2002; 76:4251–4259. [PubMed: 11932390]
45. Liu F, Whitton JL, Slifka MK. The rapidity with which virus-specific CD8+ T cells initiate IFN-gamma synthesis increases markedly over the course of infection and correlates with immunodominance. J Immunol. 2004; 173:456–462. [PubMed: 15210805]

46. Whitmire JK, Tan JT, Whitton JL. Interferon-gamma acts directly on CD8+ T cells to increase their abundance during virus infection. J Exp Med. 2005; 201:1053–1059. [PubMed: 15809350]

47. Shimizu K, Shichiri M, Libby P, Lee RT, Mitchell RN. Th2-predominant inflammation and blockade of IFN-gamma signaling induce aneurysms in allografted aortas. J Clin Invest. 2004; 114:300–308. [PubMed: 15254597]

48. King VL, Lin AY, Kristo F, Anderson TJ, Ahluwalia N, Hardy GJ, Owens AP 3rd, Howatt DA, Shen D, Tager AM, Luster AD, Daugherty A, Gerszten RE. Interferon-gamma and the interferon-inducible chemokine CXCL10 protect against aneurysm formation and rupture. Circulation. 2009; 119:426–435. [PubMed: 19139386]

49. Wang HC, Montufar-Solis D, Teng BB, Klein JR. Maximum immunobioactivity of murine small intestinal intraepithelial lymphocytes resides in a subpopulation of CD43+ T cells. J Immunol. 173:6294–6302. [PubMed: 15528368]

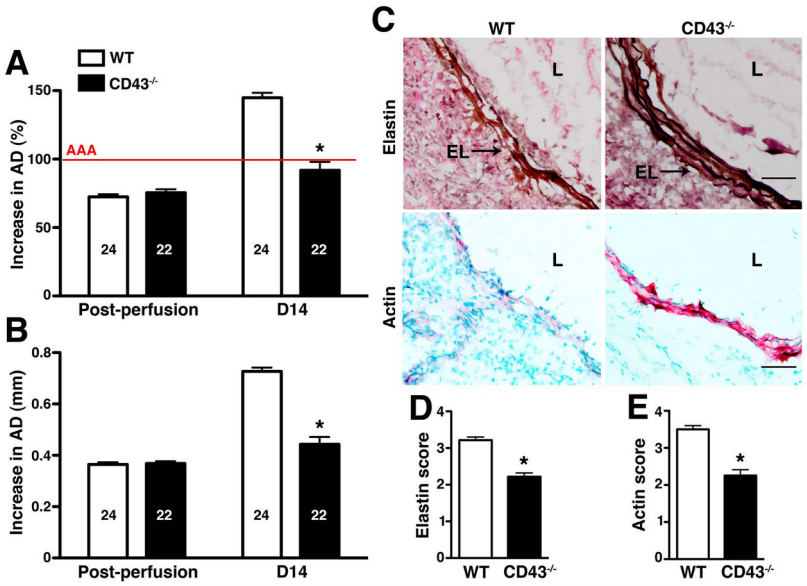

Figure 1. CD43$^{-/-}$ mice are resistant to elastase-induced AAA

WT and CD43$^{-/-}$ mice were perfused with elastase on d0 and their aortic diameter (AD) was measured immediately post perfusion and again on d14. Increase in AD was expressed in percentage (A) or mm (B). AAA (indicated by the red line in A) is defined as an increase in AD of 100% or greater over pre-perfusion parameters. Values represent mean ± SEM. The number of animals per genotype is indicated. (C) Staining for elastic fibers (upper panels) and actin content in SMCs (red stain, lower panels) showed extensive degradation of elastic fibers and depletion of SMC actin content in WT animals. D14 elastic fiber degradation (D) and SMC actin depletion (E) were graded on a scale of 1–4. Values represent mean ± SEM, n = 5 aortas per genotype. EL, elastic lamellae; L, lumen. Scale bar, 50 μm. *P < 0.0001.

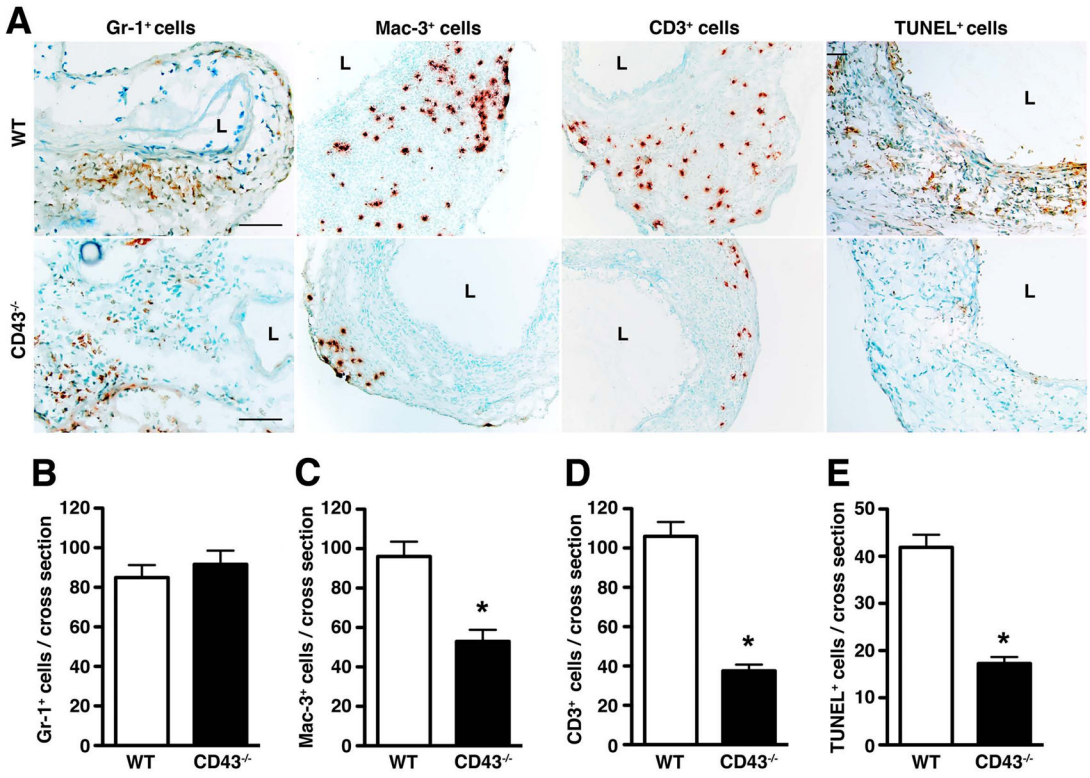

Figure 2. Absence of CD43 dampens the chronic inflammatory responses

(A) Sections of WT and CD43$^{-/-}$ aortas were stained for neutrophils (Gr-1^{+} cells), macrophages (Mac-3^{+} cells), T cells (CD3^{+} cells) and apoptotic cells (TUNEL^{+} cells). Scale bar, 100 μm. The number of Gr-1^{+} cells (B), Mac-3^{+} cells (C), CD3^{+} cells (D), and TUNEL^{+} cells (E) per aortic cross-section were enumerated. Values represent mean ± SEM; analysis was performed on 6–9 serial cross-sections per aorta, n = 4–5 aortas per genotype. *P < 0.0001.

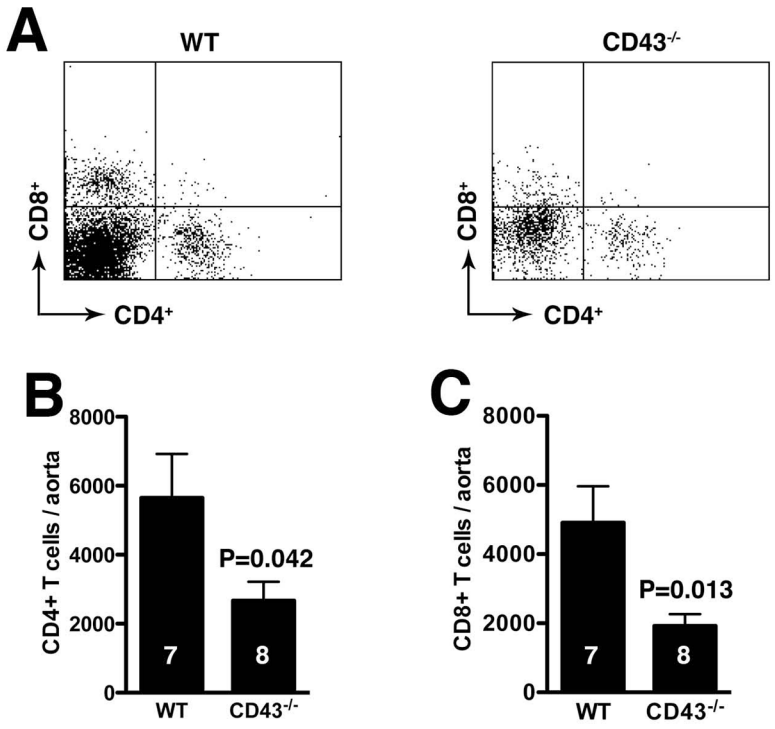

Figure 3. Dampened T cell responses in CD43$^{-/-}$ mice

WT and CD43$^{-/-}$ mice were perfused with elastase on d0 and their aortas were harvested on d14 and digested to obtained single cell suspensions. The cells were enumerated and stained with anti-CD4 and anti-CD8 mAb. CD4^{+} and CD8^{+} T cells were analyzed on CD3^{+} gated cells by flow cytometry (A). The absolute numbers of T cell subpopulations were calculated from the percentage of CD4^{+} (B) and CD8^{+} (C) cells.

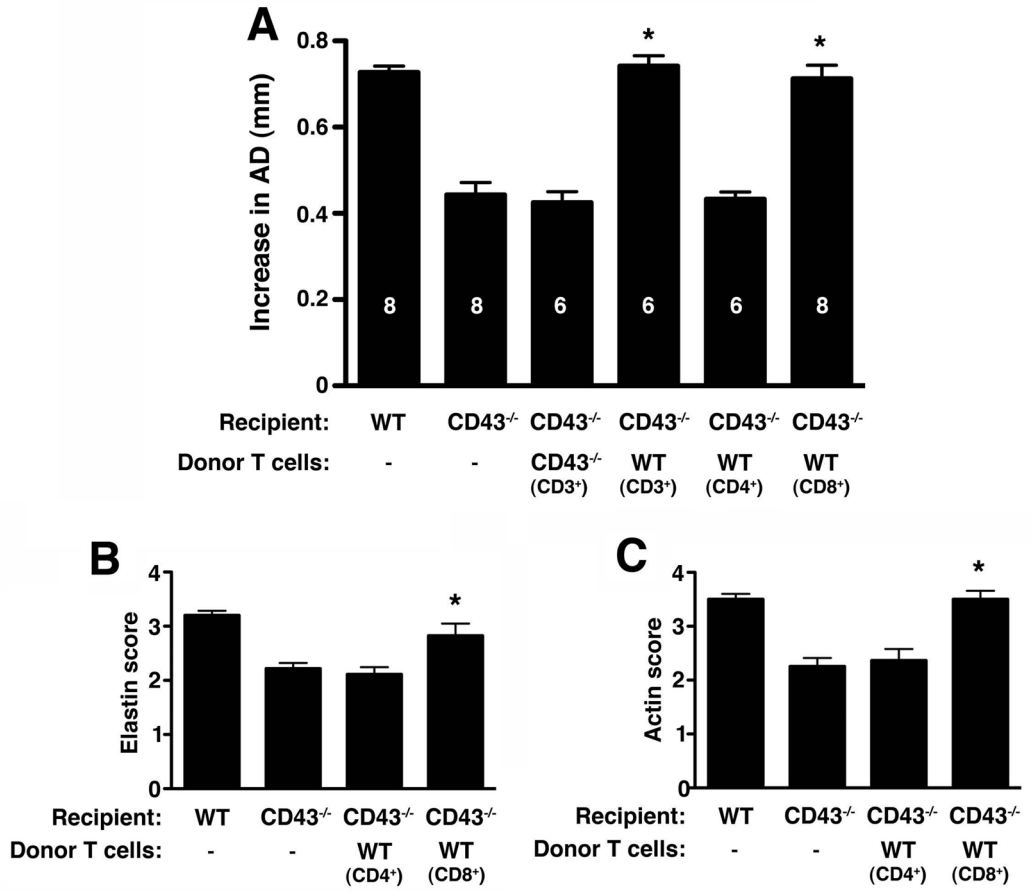

Figure 4. Reconstitution with WT CD8$^+$ T cells restores the AAA phenotype in CD43$^{-/-}$ mice

(A) Mice were perfused with elastase on d0 and received CD3$^+$, CD4$^+$ or CD8$^+$ T cells d3 and 7 where indicated. AD was measured on d14. Values represent mean ± SEM. D14 elastin degradation (B) and SMC actin depletion (C) were graded on a scale of 1–4. Values represent mean ± SEM, n = 5 aortas per genotype. *P < 0.001 compared with CD43$^{-/-}$.

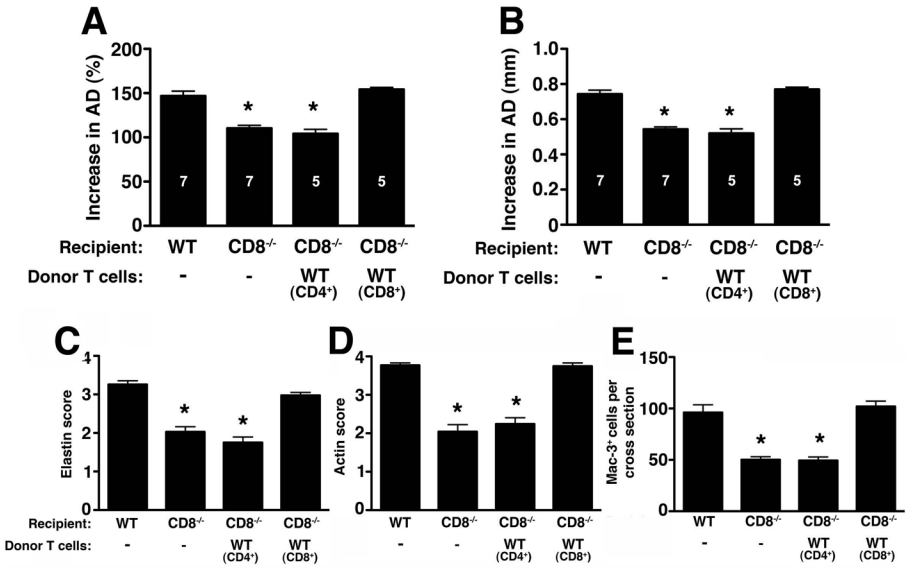

Figure 5. Absence of CD8$^+$ T cells attenuates elastase-induced AAA

Mice were perfused with elastase on d0 and increase in AD on d14 was expressed as % (A) or mm (B). Values represent mean ± SEM. D14 elastin degradation (C) and SMC actin depletion (D) were graded on a scale of 1–4; Mac-3$^+$ macrophages (E) were enumerated per aortic cross-section, n = 5 aortas per treatment. *P < 0.001 compared with WT.

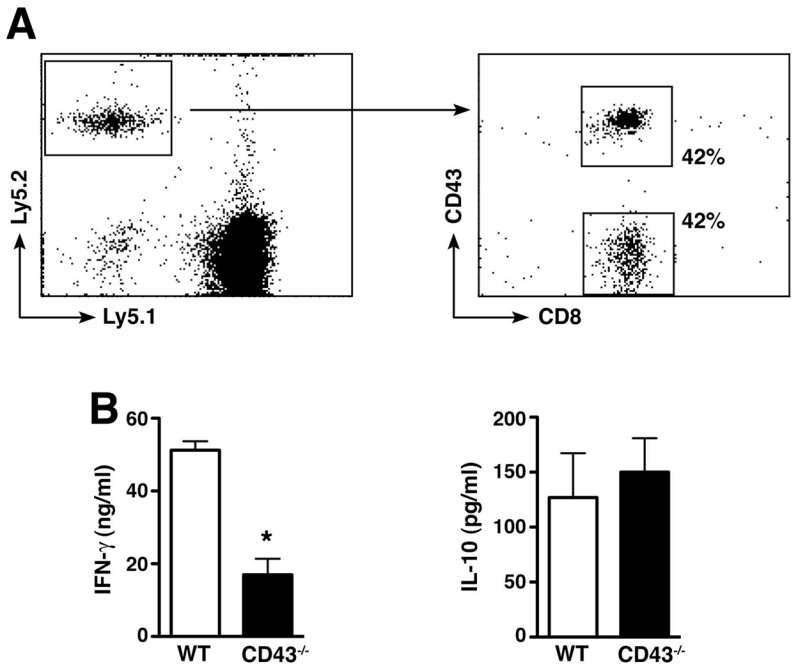

Figure 6. CD43$^{-/-}$ CD8^{+} T cell functions

(A) CD43$^{-/-}$ T cells migrate normally to site of inflammation. Ly5.2 donor WT and CD43$^{-/-}$ CD8^{+} T cells (1e7 each) were transferred into congenic Ly5.1 recipient WT mice on d1 post-elastase perfusion. On d2 cells were recovered from abdominal aorta and surface-stained for Ly5.1 vs. Ly5.2 expression. Percentage of donor CD43^{+}CD8^{+} and CD43^{-}CD8^{+} T cells were determined on Ly5.2 gated cells. (B) WT and CD43$^{-/-}$ purified CD8^{+} T cells were stimulated *in vitro* in triplicates in the presence of anti-CD23/28 mAb and IFN-γ or IL-10 released into the culture supernatant at 72 h was measured by ELISA. Values represent mean ± SEM obtained from 3 independent experiments. *P < 0.0001.

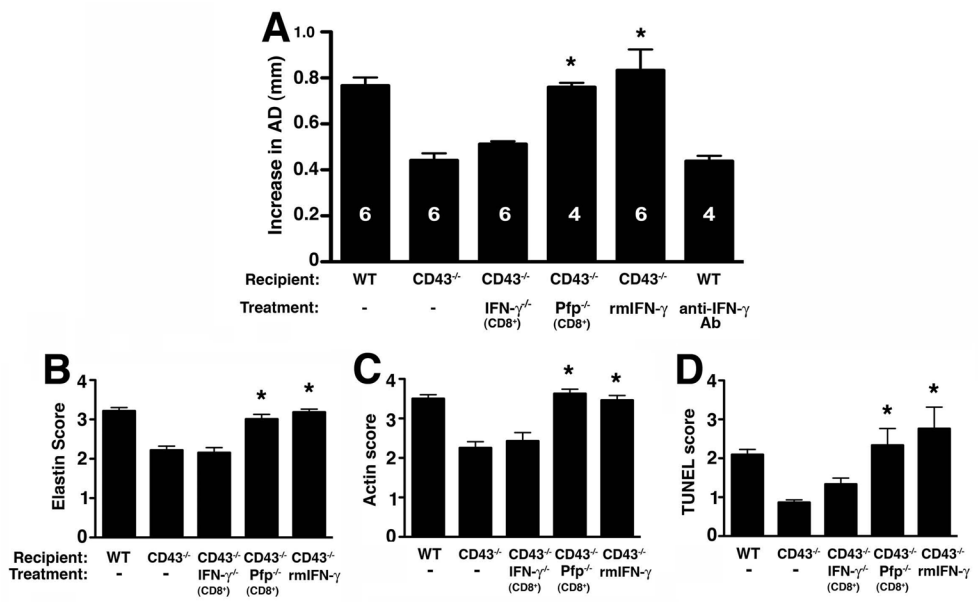

Figure 7. CD43 expression on CD8$^+$ T cells directs IFN-γ production that promotes AAA formation

(A) CD43$^{-/-}$ mice were perfused with elastase on d0 and reconstituted with IFN-γ$^{-/-}$ CD8$^+$ T cells, Pfp$^{-/-}$ CD8$^+$ T cells or administered recombinant mouse IFN-γ rmIFN-γ) or anti-IFN-γ mAb. AD was measured on d14. Values represent mean ± SEM. D14 elastin degradation (B) and SMC actin depletion (C) were graded on a scale of 1–4. (D) TUNEL$^+$ cells were enumerated per aortic cross-section. Values represent mean ± SEM, n = 5 aortas per treatment type. *P < 0.001 compared with CD43$^{-/-}$.

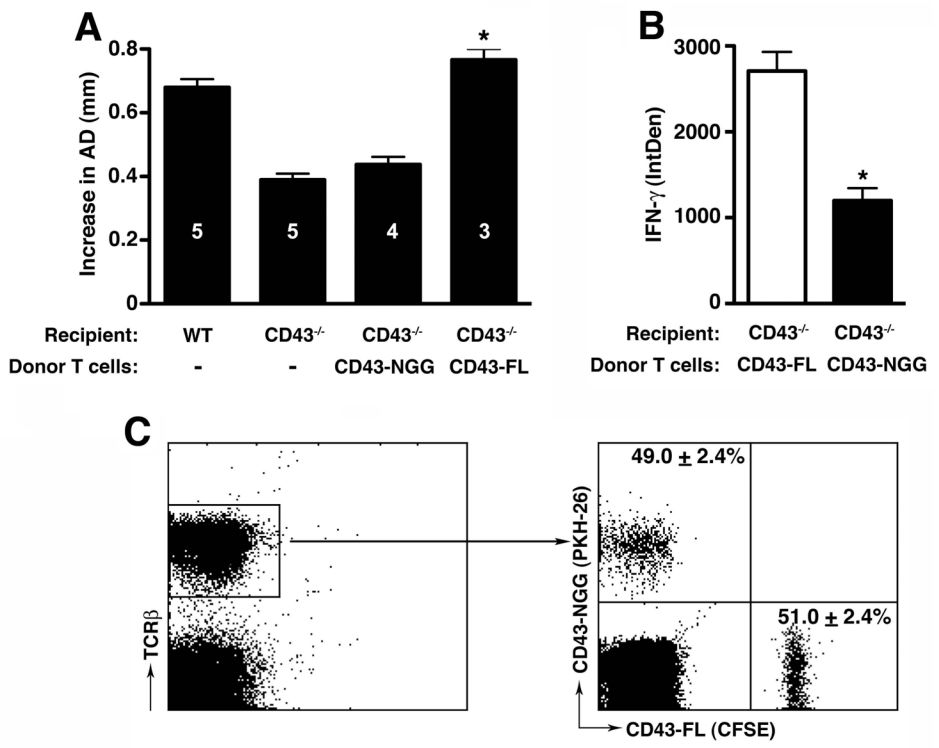

Figure 8. CD43 directs IFN-γ production in T cells through its intracellular domain

(A) CD43$^{-/-}$ mice were perfused with elastase on d0 and reconstituted with CD43-FL or CD43-NGG Tg cells on d3 and 7. AD was measured on d14. *P < 0.001 compared with non-injected CD43$^{-/-}$ animals. (B) Intracellular level of IFN-γ was analyzed using ImageJ program as detailed in the Materials and Methods section and presented as integrated optical density (IntDen). Values represent mean ± SEM, n = 3–4 aortas per genotype. *P < 0.001 compared with CD43-FL. (C) Tg cells were differentially labeled with fluorescent dyes, mixed at a 1:1 ratio and 2e7 total cells were injected i.v. into elastase perfused mice on d1; aortas were harvested on d2, digested and single cell suspensions analyzed for percentages of CFSE^{+} vs PKH-26^{+} cells in the TCRβ^{+} population. The total number of CFSE^{+} and PKH-26^{+} labeled cells (events) were added and the combined event count set at 100%. The percentage of CFSE^{+} or PKH-26^{+} cells was calculated by dividing the event counts from each fluorescent labeled population by the combined total event counts. Values represent mean ± SEM, n = 5 independent adoptive transfer experiments.

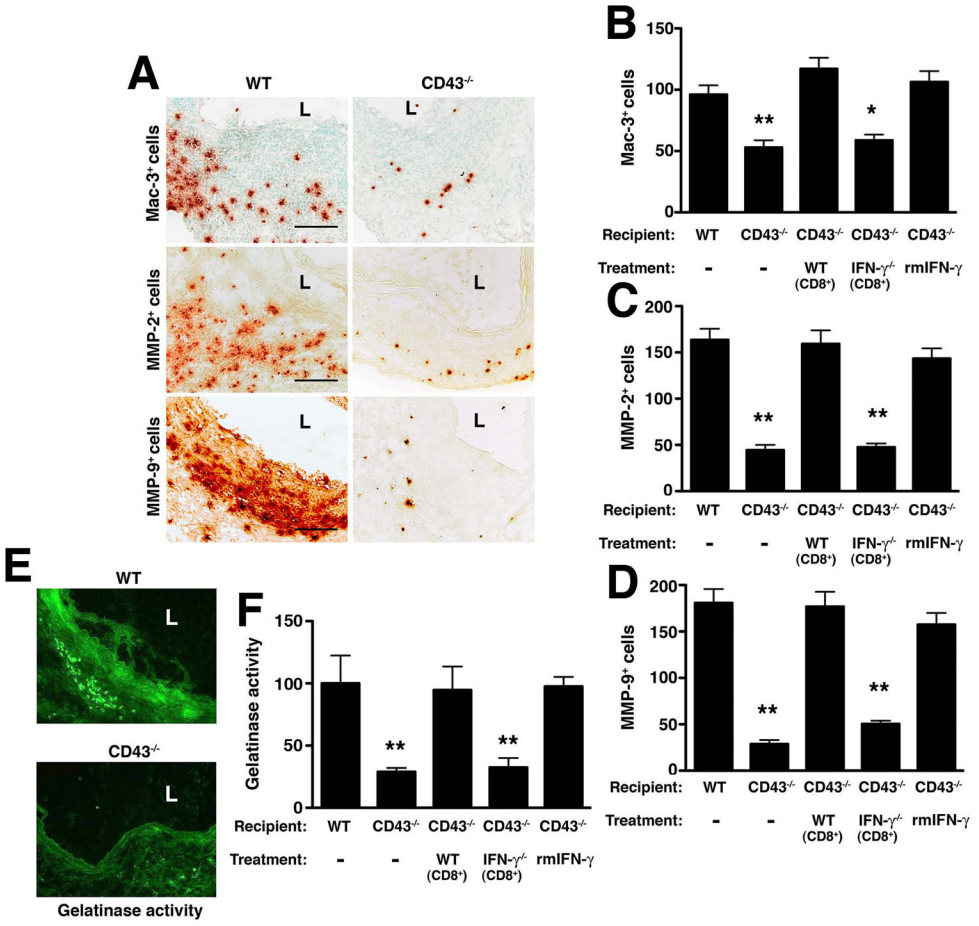

Figure 9. IFN-γ produced by CD8$^+$ T cells promotes recruitment/expansion of macrophages and MMP-producing cells

(A) D14 aortic sections from WT and CD43$^{-/-}$ mice were stained for Mac-3, MMP-2 and MMP-9. L, lumen. Scale bar, 50 μm. Mac-3$^+$ (B), MMP-2$^+$ (C) and MMP-9$^+$ (D) cells were enumerated in aortic cross sections following different treatment conditions. (E) *In situ* zymography with a fluorescein-labeled DQ gelatin substrate was used to detect the gelatinolytic activity of MMP on d14 aortic sections. (F) Images were analyzed by ImageJ software and gelatinase activity was normalized to the intensity of WT sections, which was set at 100%. Values represent mean ± SEM, n = 6–9 sections per aorta, 4–5 aortas per genotype/treatment. *P < 0.01, **P < 0.001 compared with WT.